Camera Calibration Based on the Common Self-polar Triangle of Sphere Images

Haifei Huang[1,2], Hui Zhang[2,3] and Yiu-ming Cheung[1,2]

[1] Department of Computer Science
Hong Kong Baptist University, Hong Kong
[2] United International College, BNU-HKBU, China
[3] Shenzhen Key Lab of Intelligent Media and Speech
PKU-HKUST Shenzhen Hong Kong Institution, Shenzhen, China

Abstract. Sphere has been used for camera calibration in recent years. In this paper, a new linear calibration method is proposed by using the common self-polar triangle of sphere images. It is shown that any two of sphere images have a common self-polar triangle. Accordingly, a simple method for locating the vertices of such triangles is presented. An algorithm for recovering the vanishing line of the support plane using these vertices is developed. This allows to find out the imaged circular points, which are used to calibrate the camera. The proposed method starts from an existing theory in projective geometry and recovers five intrinsic parameters without calculating the projected circle center, which is more intuitive and simpler than the previous linear ones. Experiments with simulated data, as well as real images, show that our technique is robust and accurate.

1 Introduction

Camera calibration is a fundamental task in many computer vision applications, such as motion estimation and 3D reconstruction. The main task of camera calibration is to recover the intrinsic and extrinsic parameters. Many calibration methods have been proposed in the past years. They can be classified into two categories: calibration with objects [1–3], and self-calibration [4–6].

In the first category, classical calibration techniques require the use of some highly accurate tailor-made calibration patterns, which are time-consuming and costly. To overcome this drawback, sphere has been introduced into camera calibration in recent years because sphere can be easily found in daily life and its silhouettes can be extracted reliably from image [7]. Besides, it is suitable to calibrate a camera network. As long as the sphere is placed in the common field of view of the cameras, its occluding contours are visible from any position [8].

Sphere, as a calibration target, was first used in [9] to recover the aspect ratio of the two images axes. Later, some nonlinear methods for estimating more camera intrinsic parameters had been presented. In [10], under the assumption of a zero-skew camera, a multi-step nonlinear approach to estimating four intrinsic parameters was presented. In [11], the relation of the image of absolute

conic to the image of sphere was well investigated and camera intrinsic parameters were recovered by minimizing the reprojection errors nonlinearly. In [8], a semi-definite programming approach was introduced based on the dual representation of the sphere image. However, there are some problems in nonlinear methods. In [10], error is accumulated seriously in the separated steps. In [11], an appropriate initialization should be given before stating the minimization process. In [8], when noise is large, there could be no solution sometimes. To avoid these deficiencies, from Year 2005, some linear approaches had been introduced. Zhang et al.[12, 13], treated two spheres as a surface of revolution [14] and recovered internal parameters by using pole-polar constraints on the image of absolute conic. Ying and Zha [15] interpreted the same constraint presented in [8] and [11] geometrically, and presented two linear approaches to calibrating the camera by using double contact points and double-contact theorem. Zhao and Liu [16] developed a method by treating a sphere as a revolving stick. Recently, Wong [17] has introduced a stratified approach to recovering extrinsic parameters and intrinsic parameters by finding special point correspondences. Note that the first calibration method presented in [15], as well as methods presented in [8, 16], require calculating the projected circle center at the very beginning.

In this paper, we solve the problem of camera calibration using spheres in a new perspective. We investigate the common self-polar triangle of sphere images thoroughly and find that vanishing line of the support plane can be determined by the vertices of such triangles. This allows to find out the imaged circular points, which are used to calibrate the camera. From this perspective, calculating the projected circle center at the very beginning is not necessary and conic homography theory can be interpreted as using the self-dual triangle of sphere images. Note that the proposed method is totally different from the calibration method in [13]. In [13], they investigated the plane formed by the camera center and two sphere centers. They tried to recover the vanishing line of the plane and vanishing point of the plane's normal, while our method is trying to recover the vanishing line of the support plane.

The remainder of this paper is organized as follows. Section 2 briefly introduces some notations and basic equations. Section 3 discusses the common self-polar triangle of two conics. Section 4 presents our novel calibration method. Section 5 shows the experimental results of the proposed method on synthetic and real data sets. Finally, a conclusion is drawn in Section 6.

2   Notations and Basic Equations

2.1   The Camera Model

The pinhole camera model is adopted in this paper. In the homogenous coordinate system, let $\mathbf{M} = [X\ Y\ Z\ 1]^{\mathbf{T}}$ be a world point and $\mathbf{m} = [x\ y\ 1]^{\mathbf{T}}$ be its image. The imaging process can be represented as

$$u\mathbf{m} = \mathbf{K}[\mathbf{R}|\mathbf{t}]\mathbf{M} \qquad (1)$$

where u is a nonzero scale factor, $\mathbf{R}|\mathbf{t}$ denotes a rigid transformation, and $\mathbf{K}$ is the intrinsic parameter matrix with the following format:

$$\mathbf{K} = \begin{bmatrix} \alpha f & s & u_0 \\ 0 & f & v_0 \\ 0 & 0 & 1 \end{bmatrix} \tag{2}$$

In the matrix $\mathbf{K}$, f is the focal length, α is the aspect ratio, (u_0, v_0) is the principal point, and s is the skew.

2.2   The Absolute Conic

The absolute conic was first introduced by Faugeras et al. [4] for camera self-calibration. Let $\mathbf{P} = [X \ Y \ Z \ 0]^{\mathbf{T}}$ be an infinite world point, the absolute conic is formed by the points satisfying $\mathbf{P}^{\mathbf{T}}\mathbf{P} = 0$ in a plane at infinity. The image of the absolute conic ω (IAC) is the conic $\mathbf{K}^{-\mathbf{T}}\mathbf{K}^{-1}$ and its dual ω^* (DIAC) is $\mathbf{K}\mathbf{K}^{\mathbf{T}}$ [18]. Once IAC or DIAC is determined, $\mathbf{K}$ can be easily obtained by Cholesky decomposition [19].

2.3   The Sphere Image

The image of a sphere is a conic because the occluding contour of a sphere is always a circle (see Fig.1). In [8] and [13], the algebraic relation between a sphere image and the DIAC is given by

$$\beta_i \mathbf{C}_i^* = \omega^* - \mathbf{o}_i \mathbf{o}_i^{\mathbf{T}} \tag{3}$$

where i is used to indicate the sphere index, β is a nonzero scale factor, $\mathbf{C}^*$ is the dual of the sphere image, and $\mathbf{o}$ is the image of the sphere center (projected circle center). In this paper, when we consider the non-degenerate case, $\mathbf{C}^*$ is equal to $\mathbf{C}^{-1}$.

3   The Common Self-polar Triangle of Sphere Images

In this section, we show that any two disjoint sphere images have a unique common self-polar triangle and present one method to find the vertices of the common self-polar triangle.

3.1   The Pole-polar Relationship

A line $\mathbf{l}$ formed by all harmonic conjugates of point $\mathbf{x}$ with respect to a conic $\mathbf{C}$ is called the polar of $\mathbf{x}$, and point $\mathbf{x}$ is called the pole of $\mathbf{l}$. The algebraic relation between pole $\mathbf{x}$ and polar $\mathbf{l}$ with respect to a conic $\mathbf{C}$ is given by

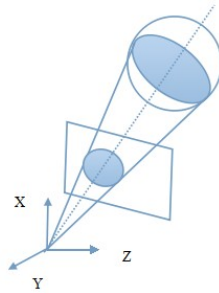$$\mathbf{x} = \mathbf{C}^{-1}\mathbf{l} \tag{4}$$

Fig. 1. Projection of a sphere

where $\mathbf{C}^{-1}$ is the dual representation of $\mathbf{C}$ [18].

If the poles of a conic form the vertices of a triangle and their respective polars form its opposite sides, it is called a self-polar triangle(see Fig.2). If a self-polar triangle is common to two conics, it is called common self-polar triangle (see Fig.3) [20].
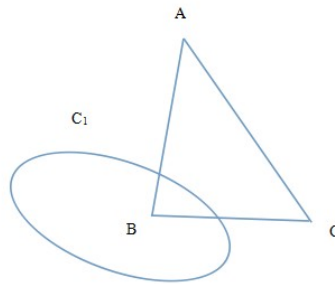

Fig. 2. $\triangle \mathbf{ABC}$ is a self-polar triangle with respect to conic $\mathbf{C}_1$ when polars of A, B and C are lines BC, AC and AB, respectively.

3.2   The Common Self-polar Triangle of Sphere Images

The relation of two conics to each other has been well studied in [20–22], especially with reference to common self-polar triangle of two conics. By considering two sphere images, we obtain the following proposition.

Proposition 1. *Two disjoint sphere images have a unique common self-polar triangle.*

Proof. In [20], there is one important theorem:
If two conics intersect in four distinct points, they have one and only one common self-polar triangle. If they are tangent in two points, they have an infinite number of common self-polar triangles, one vertex of which is at the intersection of the common tangents. In all other cases, two distinct conics have no common self-polar triangle.

Considering two disjoint conics obtained by the image of two spheres, all four intersection points are imaginary and they fall into two conjugate imaginary pairs. Obviously, four intersection points are distinct. According to the theorem mentioned above, we obtain that two disjoint sphere images have a unique common self-polar triangle. □

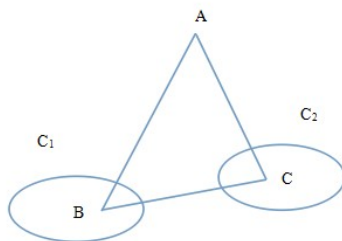**Fig. 3.** $\triangle \mathbf{ABC}$ is the common self-polar triangle of two disjoint conics $\mathbf{C}_1$ and $\mathbf{C}_2$ when $\triangle \mathbf{ABC}$ is a self-polar triangle with respect to both $\mathbf{C}_1$ and $\mathbf{C}_2$.

3.3   The Vertices of Common Self-polar Triangle

Let the two sphere images be $\mathbf{C}_1$ and $\mathbf{C}_2$, and if there exists a common pole $\mathbf{x}$ and polar $\mathbf{l}$, the following relationship should be satisfied:

$$\mathbf{l} = \mathbf{C}_1 \mathbf{x}$$
$$\mathbf{l} = \lambda \mathbf{C}_2 \mathbf{x} \tag{5}$$

where λ is a scalar parameter. Subtracting the equations in (5), we get $(\mathbf{C}_1 - \lambda \mathbf{C}_2)x = 0$. By multiplying the inverse of $\mathbf{C}_2$ on both sides, we obtain the following equation:

$$(\mathbf{C}_2^{-1}\mathbf{C}_1 - \lambda \mathbf{I})\mathbf{x} = 0 \tag{6}$$

From the equation of (6), we find the common poles for $\mathbf{C}_1$ and $\mathbf{C}_2$ are the eigenvectors of $\mathbf{C}_2^{-1}\mathbf{C}_1$.

4 Calibration Theory and Method

Based on the above proposition, this section introduces a linear approach to solving the problem of calibration.

4.1 Vanishing Line Recovery

By using the vertices of common self-polar triangle of sphere images, vanishing line of the support plane for the occluding contour can be easily recovered.

Proposition 2. *Let $\mathbf{C}_1$, $\mathbf{C}_2$ and $\mathbf{C}_3$ be the images of three spheres $\mathbf{S}_1$, $\mathbf{S}_2$ and $\mathbf{S}_3$, $\triangle\mathbf{ABC}$ be the common self-polar triangle of $\mathbf{C}_1$, $\mathbf{C}_3$, and $\triangle\mathbf{DEF}$ be the common self-polar triangle of $\mathbf{C}_1$, $\mathbf{C}_2$, the vanishing line of the support plane for the occluding contour of $\mathbf{S}_1$ is the line $\mathbf{AD}$.*

Proof. In Fig.4, $\triangle\mathbf{ABC}$ is the common self-polar triangle of $\mathbf{C}_1$, $\mathbf{C}_3$, $\triangle\mathbf{DEF}$ is the common self-polar triangle of $\mathbf{C}_1$, $\mathbf{C}_2$. Let $\mathbf{O}_1, \mathbf{O}_2$ be the imaged sphere centers of $\mathbf{S}_1$, $\mathbf{S}_2$. Multiplying the line $\mathbf{l} = \mathbf{O}_1 \times \mathbf{O}_2$ joining the images of the 2 sphere centers to both sides of (3) gives

$$\beta_1 \mathbf{C}_1^{-1} \mathbf{l} = \omega^{-1} \mathbf{l}$$
$$\beta_2 \mathbf{C}_2^{-1} \mathbf{l} = \omega^{-1} \mathbf{l} \qquad (7)$$

Let $\beta_1 \mathbf{C}_1^{-1} \mathbf{l} = \beta_2 \mathbf{C}_2^{-1} \mathbf{l} = \mathbf{x}$, we have that $\mathbf{x}$ and $\mathbf{l}$ are the common pole and polar of $\mathbf{C}_1$, $\mathbf{C}_2$. Based on this, in Fig.4, it is easy to find that line $\mathbf{EF}$ goes through $\mathbf{O}_1, \mathbf{O}_2$. Similarly, line BC goes through $\mathbf{O}_1, \mathbf{O}_3$. Since $\mathbf{A}$ is the pole of BC and $\mathbf{D}$ is the pole of $\mathbf{EF}$, we have that $\mathbf{A}$ and point $\mathbf{D}$ are all harmonic conjugates of $\mathbf{O}_1$ with respect to $\mathbf{C}_1$. According to polar definition described in Subsection 3.1, point $\mathbf{A}$ and point $\mathbf{D}$ should be on the polar of $\mathbf{O}_1$. Since point $\mathbf{O}_1$ is a projected circle center, its polar should be the vanishing line of the support plane [20]. From those two facts, we obtain that line $\mathbf{AD}$ is the vanishing line. Using the same way, vanishing lines of the support planes for the occluding contours of $\mathbf{S}_2$ and $\mathbf{S}_3$ can be recovered.   □

Here, the procedure for recovering the vanishing line of the support plane is briefly summarized below:
1. Obtain sphere images $\mathbf{C}_1$, $\mathbf{C}_2$ and $\mathbf{C}_3$.
2. Calculate vertices of the common self-polar triangle for any two sphere images using (6).
3. Find vertices outside of the sphere images and connect any two of them.

4.2 Calibration Method

As we all know, any circle intersects line at infinity of the support plane in the circular points and circular points lie on the absolute conic. Accordingly, in the image plane, the imaged circular points lie on IAC [18]. If the image of the circle
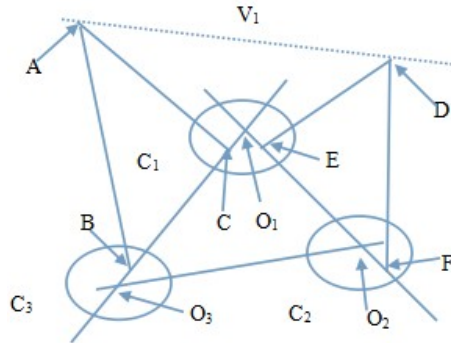
Fig. 4. Vanishing line recovered from vertices of common self-polar triangle of sphere images.

and image of line at infinity are both obtained, we can calculate the images of the two circular points. One pair of imaged circular points provides two independent constraints on IAC. Hence three pairs are needed to fully calibrate. Given three sphere images, we can easily find the self-polar triangle for any two of them. Based on the propositions above, three vanishing lines can be detected and the image of the circular points can be calculated. Consequently, a camera can be calibrated.

The complete calbration algorithm by using the common self-polar triangles of sphere images consists of the following steps:
1. Obtain sphere images $\mathbf{C}_1$, $\mathbf{C}_2$ and $\mathbf{C}_3$.
2. Recover three vanishing lines by using common self-polar triangles.
3. Find the imaged circular points, and then determine ω and obtain $\mathbf{K}$ using the Cholesky factorization.

5   Experiments and Results

5.1   Synthetic Data

In the computer simulations, the synthetic camera has focal length $f = 600$, aspect ratio $\alpha = 1.1$, skew $s = 0.1$, and principal point $(u_0, v_0) = (320, 240)$. The image resolution is: 800×600. An image containing three sphere images is generated. They are uniformly distributed within the image. We choose 500 points on each sphere image, and gaussian noise with zero-mean and σ standard deviation is added to these image points. Ellipses are fitted to these images using a least squares ellipse fitting algorithm. In our experiment, we compare our proposed approach with a nonlinear semi-definite approach presented in [8] and a linear orthogonal approach presented in [13]. To evaluate accuracy and robustness of these methods, we vary the noise level σ from 0 to 6 pixels, and perform 15 independent trials, 30 independent trials as well as 50 independent trials for each

noise level. The mean values of these recovered parameters are computed over each run. The average percentage errors of f are shown in Fig. 5. The errors of other parameters, which are not shown here, exhibit similar trend. It can be seen that the errors increase linearly with the the noise level and our method performed as well as others.

Note that the results between our approach and orthogonal approach are very similar. When we calculate the average percentage errors, they are almost the same. That explains why the curves of these two approaches in Fig.5 are overlapped. In order to show the little difference clearly, estimated parameters under different noise level with 50 trials are shown in Table.

**Table 1.** Experimental results with 1 pixel noise(50 trials)

Approach	αf	f	s	u_0	v_0
Ground-truth	660	600	0.1	320	240
Semi-definite(nonlinear)	655.3167	595.7662	1.9698	319.6274	238.4794
Orthogonal(linear)	655.2565	595.7586	2.0010	319.8414	238.3899
Our approach(linear)	655.2565	595.7192	2.7449	319.8750	238.6999

**Table 2.** Experimental results with 2 pixels noise (50 trials)

Approach	αf	f	s	u_0	v_0
Ground-truth	660	600	0.1	320	240
Semi-definite(nonlinear)	649.4490	590.3716	3.5963	320.5770	239.1416
Orthogonal(linear)	649.5920	590.5997	3.7439	320.3166	238.6542
Our approach(linear)	649.5920	590.3723	3.9832	320.6633	233.1286

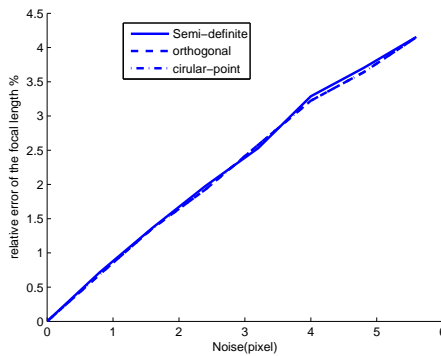**Table 3.** Experimental results with 3 pixels noise (50 trials)

Approach	αf	f	s	u_0	v_0
Ground-truth	660	600	0.1	320	240
Semi-definite(nonlinear)	643.8556	585.5044	5.0356	323.2800	236.9793
Orthogonal(linear)	643.8120	585.4920	4.9911	322.3709	237.8458
Our approach(linear)	643.8120	582.6786	3.4279	324.3849	241.1814
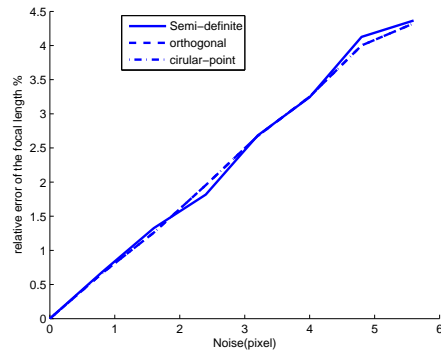
(a)
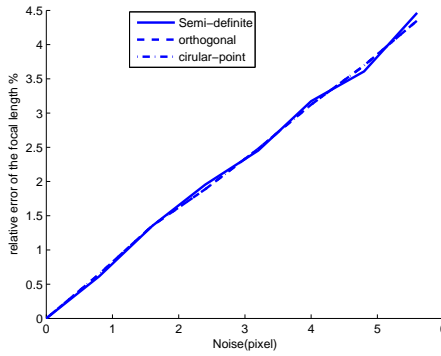
(b)

(c)

Fig. 5. (a) The estimated results with 15 trials. (b) The estimated results with 30 trials. (c) The estimated results with 50 trials. Due to the results of our approach(Circular-point) and orthogonal approach have little difference, the curves of these two approaches almost overlap.

5.2   Real Scene

In the real scene experiment, we used 3 plastic balls as calibration objects. Real images were taken with a Canon EOS5D CCD camera. The image resolution is 720×480. The images of spheres were extracted using Canny's edge detector [23], and ellipses are fitted to these images using a least squares ellipse fitting algorithm. The camera is calibrated with the proposed approach, and results are compared with semi-definite approach as well as orthogonal approach. The estimated parameters are listed in Table 4, where the result from the classical method of Zhang [2] is taken as the ground truth. Fig.6b shows the calibration pattern used as ground truth.

(a)   (b)

Fig. 6. (a) Image of three balls. (b) Image of calibration pattern.

Table 4. Real experiment results

Approach	αf	f	s	u_0	v_0
Zhang(ground truth)	1070	1070	0	359	239
Semi-definite(nonlinear)	1107	1108	1.07	352	230
Orthogonal(linear)	1130	1131	1.19	353	232
Our method(linear)	1121	1122	1.05	352	231

5.3   Critical Configuration

Note that in some situations, the calibration process fails. First, when spheres placed near the image centers, the vanishing line of the support plane will be far away from the image center, which will be recovered badly. Second, when any two of the support planes are parallel, less constraints can be obtained and the camera can not be calibrated. However, those situations can be avoided by carefully placing spheres.

6   Conclusion

We have proposed a very simple calibration algorithms based on the common self-polar triangles of sphere images, by using a single image of at least three spheres. We have shown how to locate the vertices of the common self-polar triangle and how to recover the vanishing line of the support plane. All computations involved are linear and simple. The experimental results have demonstrated that the proposed method is accurate and robust. Nevertheless, this paper has yet to consider the distortion problem, which will leave for our future studies.

References

1. Tsai R.Y.: A versatile camera calibration technique for high accuracy 3d machine vision metrology using off-the-shelf tv cameras and lenses. IEEE Journal of Robotics and Automation **3** (1987) 323–344
2. Zhang Z.: A flexible new technique for camera calibration. IEEE Trans. on Pattern Analysis and Machine Intelligence **22** (2000) 1330–1334
3. Zhang Z.: Camera calibration with one-dimensional objects. IEEE Trans. on Pattern Analysis and Machine Intelligence **26** (2004) 892–899
4. Faugeras O.D., Luong Q.-T., Maybank S.J.: Camera self-calibration: Theory and experiments Proc. ECCV (1992) 321–334
5. Hartley R.: An algorithm for self calibration from several views. IEEE Conference on Computer Vision and Pattern Recognition (1994) 908–912
6. Maybank S.J., Faugeras O. D.: A theory of self-calibration of a moving camera. International Journal of Computer Vision **8** (1992) 123–151
7. Fitzgibbon A. W., Pilu M., Fisher R. B.: Direct least-squares fitting of ellipses. IEEE Trans. on Pattern Analysis and Machine Intelligence **21** (1999) 476–480
8. Agrawal M., Davis L. S.: Camera calibration using spheres: A semi-definite programming approach. Proc. of IEEE International Conf. on Computer Vision (2003) 782–789
9. Penna M. A.: Camera calibration: A quick and easy way to determine the scale factor. IEEE Trans. on Pattern Analysis and Machine Intelligence **13** (1991) 1240–1245
10. Daucher D., Dhome M., Lapreste J.: Camera calibration from spheres images. Proc. ECCV (1994) 449–454
11. Teramoto H., Xu G.: Camera calibration by a single image of balls: From conics to the absolute conic. Proc. of 5th ACCV (2002) 499–506
12. Zhang H., Zhang G., Wong K.-Y. K.: Camera calibration with spheres: Linear approaches. Proc. International Conference on Image Processing **2** (2005) 1150–1153
13. Zhang H., Zhang G., Wong K.-Y. K.: Camera calibration from images of spheres. IEEE Trans. on Pattern Analysis and Machine Intelligence **29** (2007) 499–503
14. Wong K.-Y. K., Mendonça P. R. S., Cipolla R.: Camera calibration from surfaces of revolution. IEEE Trans. on Pattern Analysis and Machine Intelligence **25** (2003) 147–161

15. Ying X., Zha H., Geometric interpretations of the relation between the image of the absolute conic and sphere images. IEEE Trans. on Pattern Analysis and Machine Intelligence **28** (2006) 2031–2036
16. Zhao Z., Liu Y.: Applications of projected circle centers in camera calibration. Machine Vision and Applications **21** (2010) 301–307
17. Wong K.-Y. K., Zhang G., Chen Z.: A stratified approach for camera calibration using spheres. IEEE Trans. on Image Processing **20** (2011) 305–316
18. Hartley R.I., Zisserman A.: *Multiple View Geometry in Computer Vision*. Cambridge University , UK (2000)
19. Gentle J.E.: *Numerical Linear Algebra for Applications in Statistics*. Springer-Verlag, (1998)
20. Frederick S. Woods: *Higher Geometry*. Ginn and Company, USA (1922)
21. Filon L.N.G.: *Introduction to Projective Geometry*. Edward Arnold, UK (1908)
22. Semple J.,Kneebone G.: *Algebraic Projective Geometry*. Oxford Science, UK (1952)
23. Canny J.: A computational approach to edge detection IEEE Trans. on Pattern Analysis and Machine Intelligence **8** (1986) 679–698